*Environ. Sci. Technol.* **2010,** *44,* 2072–2078

# Stream Temperature Response to Three Riparian Vegetation Scenarios by Use of a Distributed Temperature Validated Model

T. R. ROTH,*,† M. C. WESTHOFF,‡ H. HUWALD,§ J. A. HUFF,† J. F. RUBIN,|| G. BARRENETXEA,§ M. VETTERLI,⊥ A. PARRIAUX,§ J. S. SELKER,† AND M. B. PARLANGE§

*Department of Water Resource Engineering, Oregon State University, 116 Gilmore Hall, Corvallis, Oregon 97331, Water Resources Section, Faculty of Civil Engineering and Geosciences, Delft University of Technology, Post Office Box 5048, 2600 GA Delft, The Netherlands, School of Architecture, Civil and Environmental Engineering and School of Computer and Communication Sciences, Ecole Polytechnique Fédérale de Lausanne, Lausanne, Switzerland, and University of Applied Sciences of Western Switzerland, 150 route de Presinge, Jussy, Switzerland*

*Received September 8, 2009. Revised manuscript received January 5, 2010. Accepted January 25, 2010.*

Elevated in-stream temperature has led to a surge in the occurrence of parasitic intrusion proliferative kidney disease and has resulted in fish kills throughout Switzerland's waterways. Data from distributed temperature sensing (DTS) in-stream measurements for three cloud-free days in August 2007 over a 1260 m stretch of the Boiron de Morges River in southwest Switzerland were used to calibrate and validate a physically based one-dimensional stream temperature model. Stream temperature response to three distinct riparian conditions were then modeled: open, in-stream reeds, and forest cover. Simulation predicted a mean peak stream temperature increase of 0.7 °C if current vegetation was removed, an increase of 0.1 °C if dense reeds covered the entire stream reach, and a decrease of 1.2 °C if a mature riparian forest covered the entire reach. Understanding that full vegetation canopy cover is the optimal riparian management option for limiting stream temperature, in-stream reeds, which require no riparian set-aside and grow very quickly, appear to provide substantial thermal control, potentially useful for land-use management.

## Introduction

Land-use management practices have long been shown to play a prominent role in maintaining appropriate in-stream temperatures for aquatic species (*1*−*3*). Fish habitat has undergone degradation from direct anthropogenic and climate change effects (*4*). This has threatened many fish populations, requiring adaptive water resource management policies that provide adequate habitat for the survival of native fish. Cold water aquatic species, such as salmonids, have shown high mortality rates when stream temperature thresholds are exceeded, primarily due to impaired growth and increased predation rates (*5*−*9*). Therefore, a quantitative understanding of stream temperature response to management practices is vitally needed.

Solar radiation is often the most significant physical control on stream temperature that is amenable to management and land-use practices (*9*−*13*). An increase in riparian vegetation reduces solar radiation absorbed by the water, lowering maximum water temperatures. Due to the possibility of reducing the loss of longwave radiation at night, the effect of vegetation on, and the biological implications of, minimum stream temperature response is less straightforward (*14, 15*). However, diurnal fluctuations are important to the natural system, leading us to conclude that maxima as well as minima are relevant to habitat health. Riparian vegetation loss can increase other processes that play a role in heat exchange between the atmosphere and water surface, for example, by increasing wind speed and decreasing relative humidity (*10, 16, 17*). The lack of vegetation presence correlates with an increase in land surface temperature, which may impact local near-stream air mass transfer (*18*). Recent research on the effects of riparian vegetation on stream temperature alterations from solar radiation loading have focused, in part, on shading effects (*10, 19, 20*). Johnson (*10*) suggested that shading can have a muting effect on diurnal stream temperatures. Larson and Larson (*19*) concluded that the ability of a stream to resist temperature increases depends largely on the volume of water in the stream and the proximity of the vegetation to the stream, that is, the capacity to protect the exposed stream area from solar radiation. While intuitively reasonable, these prescriptions are largely qualitative and of limited use in rational selection between competing management options.

In this paper we modeled temperature response behavior of a segment of the Boiron de Morges River in southwest Switzerland to various riparian vegetation covers. We employed a physically based, one-dimensional temperature model coupled with distributed temperature sensing (DTS) technology and integrated on-site environmental measurement stations to validate the model outputs. Using these techniques, we attempt to answer three fundamental restoration questions regarding in-stream temperature: (1) What are the most advantageous sets of riparian land use management practices to achieve design goals, specifically peak in-stream temperatures? (2) What are the expected impacts of a selected set of restorative actions, that is, riparian vegetation cover type? (3) Are predictive models using integrated meteorological measurements and DTS as validation techniques a useful approach to accurately assess stream restoration project success?

## Materials and Methods

**Site Description, Data Collection, and Model Explanation.** Located in the southwest of Switzerland, the Boiron de Morges River is a 14-km stream fed from the Jura Mountains draining into Lake Geneva. Much of the upper stream channel has been straightened and modified as a result of the extensive history of agricultural presence in the region. The Boiron watershed includes 132 active farms cultivating a total of 1959 ha. Cereals, corn, oleaginous plants, and wine grapes are the primary crops of the region (*21*). Due to the intensive agricultural land use and the proximity to this important

* Corresponding author phone: (541)737-6314; fax: (541)737-2082; e-mail: rothtra@engr.orst.edu.
† Oregon State University.
‡ Delft University of Technology.
§ School of Architecture, Civil and Environmental Engineering, Ecole Polytechnique Fédérale de Lausanne.
|| University of Applied Sciences of Western Switzerland.
⊥ School of Computer and Communication Sciences, Ecole Polytechnique Fédérale de Lausanne.


10.1021/es902654f

Published on Web 02/04/2010

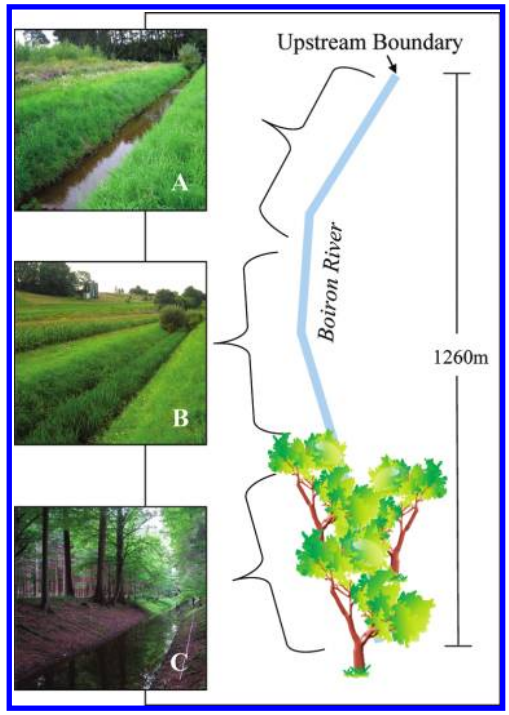


**FIGURE 1. Study reach with predominant vegetation cover type shown. (A) Open section, 0−340 m, (B) reed section, 340−860 m, and (C) forest section, 860−1260 m.**

lake, this watershed has been the focus of recent environmental research (*22*−*24*), including a large-scale 5-year multidisciplinary effort that specifically addressed the decline in fish catch within Switzerland's waterways (*25*).

Stream temperatures have been shown to have significant effect on fish populations within the Boiron. Many rivers in Switzerland have experienced a 1.5−2 °C increase in maximum annual water temperatures over the last 20 years, partly due to riparian zones lacking adequate solar radiation buffering capacity, the effect of hydroelectric power stations, and sewage treatment effluent (*26*). Temperature increases also have increased the occurrence of stream parasites and pathogens that adversely affect fish populations. Sustained in-stream temperatures greater than 15 °C are associated with proliferative kidney disease (PKD) in trout species, caused by the parasite *Tetracapsuloides bryosalmonae* (*27*).

During a 3-day period from August 11 to 13, 2007, a 1260 m reach was chosen as our study site on the basis of the presence of both threatened fish species and three distinct vegetation cover types that span the range of possible stream-side treatments under consideration (Figure 1). Additionally, in August the stream is subject to peak ambient air temperatures and this is when the stream experiences its highest in-stream temperatures of the year, thus allowing us to evaluate vegetation cover effects on stream temperature with greater confidence. At the upstream stream measurement boundary from 0 to 340 m, the stream channel was open water with scattered shrub vegetation along the banks. From 340 to 860 m there was significant in-stream reed growth but without significant bank vegetation. The 860−1260 m section was covered by a mature deciduous forest. These sections are referred to as open, reeds, and forest. The open and reed sections had small concrete segments embedded within the substrate, estimated to cover a third of the exposed streambed. These blocks contribute to the thermal conductivity of the soil and are taken into account in the energy balance equations. Stream flow during the study period was 82.5 L/s, with slight fluctuations due to irrigation pumping. The stream cross-section is trapezoidal with stream channel width ranging from 2.10 to 3.75 m with a mean of 3.07 m, with mean water depths for the open, reeds, and forest sections of 0.29, 0.58, and 0.47 m, respectively.

**TABLE 1. Calibrated Values of $D_f$ and $\theta_{vts}$ for the Three Land Use Types along the Studied Stretch of the Boiron River**

| distance (m) | land use | depth (m) | $D_f$ | $\theta_{vts}$ |
|---|---|---|---|---|
| 0−160 | open | 0.2 | 0.40 | 1 |
| 160−240 | open | 0.35−0.45 | 0.35 | 1 |
| 240−340 | reeds (few) | 0.45−0.55 | 0.30 | 0.925 |
| 340−840 | reeds (dense) | 0.50−0.65 | 0.18 | 0.9 |
| 840−1260 | forest | 0.4−0.5 | 0.15 | 0.975 |

In-stream temperature measurements were taken by a DTS instrument (Agilent N4386A) set to 1.5 m spatial resolution with a trace taken every 10 min with a duplex multimode 50/125 BRUsteel fiber optic cable (Brugg Cables) placed on the bottom of the center of the stream (see refs *28and 29* for more details about DTS methods).

Meteorological data representative for the different sections of the investigated stretch of the Boiron de Morges River was obtained via an integrated wireless sensor network array, SensorScope technology (sensorscope.epfl.ch). At six locations over the course of the experiment, SensorScope stations were deployed near the stream, each measuring solar radiation, ambient air and surface temperature, relative humidity, wind speed, and wind direction at 2-min intervals at a height of 2 m.

An energy balance approach model, after Westhoff et al. (*30*), is used to simulate the temperature in the stream. The model takes into account the following fluxes: solar radiation, longwave radiation, streambed conduction, latent heat (evaporation), and sensible heat (convection). Longwave radiation includes atmospheric radiation and radiation emitted from the water column, land surface, and vegetation. The turbulent fluxes are found by use of the Penman−Monteith equation (*31*) and subsequently the Bowen ratio. Heat energy transfer between the water and the riverbed is driven by temperature differences between the water and the substrate layer. This is a layer located between the water and the deeper alluvium and is influenced by energy fluxes. Heat conduction is computed with the assumption that the river bed is saturated.

The SensorScope stations provided measurements of the necessary environmental inputs to the model. The model was calibrated by optimizing the parameters $D_{fo}$, $\theta_{vts}$, and $T_s$ by a root-mean-squares error analysis against the observed DTS output. The parameters represent the total amount of incoming shortwave radiation available at the water surface ($D_{fo}$), the view to sky coefficient ($\theta_{vts}$), and the temperature of the deeper alluvium ($T_s$), which we assume is constant at a depth of 0.2 m. $T_s$ was taken to be the same for the whole stream (9 °C), while $\theta_{vts}$ differs for each combination of stream conditions, and $D_{fo}$ was assumed to vary with land use and water depth. This resulted in five different sets of parameters representing different combinations of land use and water depth, which are present in the stream (Table 1).

$D_f$ is determined by use of a Beer's law exponential extinction equation and varies with water depth. The solar radiation intensity reaching the streambed decreases exponentially with the measured stream depth profiles as follows:

$$D_f = D_{fo}e^{-\alpha d} \quad (1)$$

where $D_f$ is the fraction of incoming shortwave radiation that penetrates the water column and goes to heating the substrate depending on the vegetation cover type as determined by the calibration procedure, α is the extinction coefficient where a mean value for water was used (0.05 $m^{-1}$) (*32*), and $d$ is stream depth (meters). In this study α is

considered a constant that reflects the water's ability to absorb and diffuse light, for example, turbidity of the stream.

The $D_f$ and $\theta_{vts}$ parameters appear in the following energy balance equations:

$$SW_d = (1 - D_f)[D_s R_{sw} + (1 - D_s)SR_m] \quad (2)$$

$$SR_b = D_f[D_s R_{sw} + (1 - D_s)SR_m] \quad (3)$$

$$LWR_l = \varepsilon(1 - \theta_{vts})\varepsilon\sigma(T_{air})^4 \quad (4)$$

where $SW_d$ is defined as the amount of incoming shortwave radiation that goes to heating the stream, $D_s$ is a constant (dimensionless) set at 0.95, representing the fraction of sunlight that is directed to the stream, $R_{sw}$ is the incoming direct beam solar radiation, corrected for shadow effects (watts per square meter), and $SR_m$ is measured solar radiation from SensorScope (watts per square meter). $SR_b$ is the substrate conduction (watts per square meter) and is defined as the amount of incoming shortwave radiation that reaches the streambed, $LWR_l$ is the longwave radiation (watts per square meter) contributed to the stream by vegetation, $\varepsilon$ is the emissivity (dimensionless) set at 0.96, and $\sigma$ is the Stephan−Boltzmann constant ($5.67 \times 10^{-8}$ W m$^{-2}$ K$^{-4}$). Temperature of the canopy is assumed to equal the measured air temperature.

The influence of the concrete block at the bottom of the stream is expressed in thermal conductivity of the riverbed ($K_s$). $K_s$ is a weighted average of $K_{sed}$, $K_w$, and $K_c$:

$$K_s = [K_{sed}(1 - \eta) + K_w\eta)](1 - B_d) + K_c B_d \quad (5)$$

where $K_{sed}$, $K_w$, and $K_c$ are the thermal conductivity (watts per meter per degree Celsius) of the sediment, the water, and the concrete layer, respectively. Soil porosity $\eta$ (dimensionless) is set at 0.3, and $B_d$ is the relative distribution (dimensionless) of $K_c$ and determines the concrete portion in the $K_s$ term. The concrete blocks within the bottom of the stream are reflected in the $K_s$ term and play an important role in the soil energy flux, especially in the shallow part of the stream where the velocity is higher and no sediments cover the concrete, leaving the concrete exposed to solar radiation heating. We estimated an initial $B_d$ value of 0.50 that is velocity-dependent; that is, in the high-velocity portion of the stream there is no sediment covering the concrete and therefore the relative distribution of concrete to sediment is 0.50. This value is based on in-field observations of the concrete area relative to sediment in the riverbed. Total bed conduction is defined as the cumulative effect of thermal heating of the stream by the volumetric thermal conductivity of the substrate conduction layer ($K_s$) and the amount of solar radiation available for substrate conduction ($SR_b$).

Observed DTS data were used to calibrate and validate the energy balance stream temperature model and as upstream boundary conditions for each section. Once a suitable calibration was found by a parameter sensitivity analysis, we ran three simulations to explore the impact of vegetation on stream temperature, using an identical temporal resolution as the calibrated model: (1) open, where all reeds and trees were removed; (2) reeds, where the entire stream was simulated as being fully vegetated with in-stream reeds; and (3) forest, wherein the entire stream was assumed to be under a closed-canopy forest. The open scenario was simulated by using the meteorological inputs, that is, air temperature, and the calibrated model parameters found within the 0−340 m section in the calibrated model, which were then applied to the entire reach length. The reeds scenario used the values found in the 340−860 m section of the reach, while the forest scenario used the values found within the 860−1260 m reach (Table 1).

In the dense reeds part of the calibrated model, the observed velocity of the propagation of heat downstream during the diurnal cycle is faster than the velocity of the water itself. To account for this effect, we assumed a smaller effective cross-sectional area due to the dense reeds, which results in a higher stream velocity. A reduction of 10% in the cross-sectional area appeared to be sufficient to explain the higher heat wave velocity.

## Results and Discussion

To evaluate stream temperature response to riparian vegetation cover, we calculated four summary statistics related to temperature extremes: mean peak, mean minimum, absolute maximum, and absolute minimum. We examined the modeled temperature differences using these metrics for the three vegetation cover types.

Mean peak temperatures were calculated from a 2-h time period, 2:30−4:30 p.m. for mean maximum and 4:30−6:30 a.m. for mean minimum. Spatially, the mean temperatures were calculated at the downstream boundary of the stream for each scenario. The rationale was that, at the downstream boundary, the mean peak in-stream temperature should be an indicator of the stream temperature response to the integrated upstream influences on the stream. The presence of endangered fish species directly downstream from this section of the Boiron de Morges River also makes this a preferred choice. Absolute temperature maxima are relevant because some freshwater biota are susceptible to changes in average temperature, while others are limited by a maximum temperature threshold. Mean minimum temperatures can expose effects of substrate on stream temperatures and subsurface mixing.

The control simulation, that is, calibrated model output, provided an output that corresponded well to observed DTS measurements, resulting in a RMSE of 0.21 °C (Figure 2). Mean stream velocities varied from 0.076 m/s for the open and forest scenarios to 0.072 m/s for the reeds, resulting in hydraulic residence times of 4.6−4.9 h, respectively. Results from the various vegetation cover simulations reinforced expectations that a forest canopy cover reduces peak temperatures while an open system corresponds to increases in peak temperatures. The forest scenario provided a reduction of 1.2 °C and the open scenario a 0.7 °C increase of peak temperatures (Figure 3). The simulated reeds scenario predicted a 0.1 °C increase in mean maximum stream temperature compared to the calibrated model simulation. The reeds provided 32% of the decrease in peak temperatures seen between open and forest simulations (Table 4). These results indicate that in-stream reeds have a significant capacity to limit the stream's maximum temperature. Minimum stream temperatures were unaffected by the three riparian vegetation scenarios tested. The entire range of simulations shows differences in minimum temperature of less than 0.3 °C, with the forest simulation having the lowest night-time temperature and reeds the highest (Table 4). The lack of vegetation cover in the open scenario leads to radiative cooling from reducing the amount of longwave radiation into the stream and allows slightly higher evaporation rates.

Consideration of the solar radiation energy balance affecting the stream is useful in understanding these results (Table 3). Surface-emitted longwave radiation and atmospheric longwave radiation loads are not altered in any considerable way for each of our simulations and, in general, cancel each other out. Differences in substrate conduction are explained by $D_f$ distribution in eq 3. Relative differences in the evaporative flux between simulations relate to the

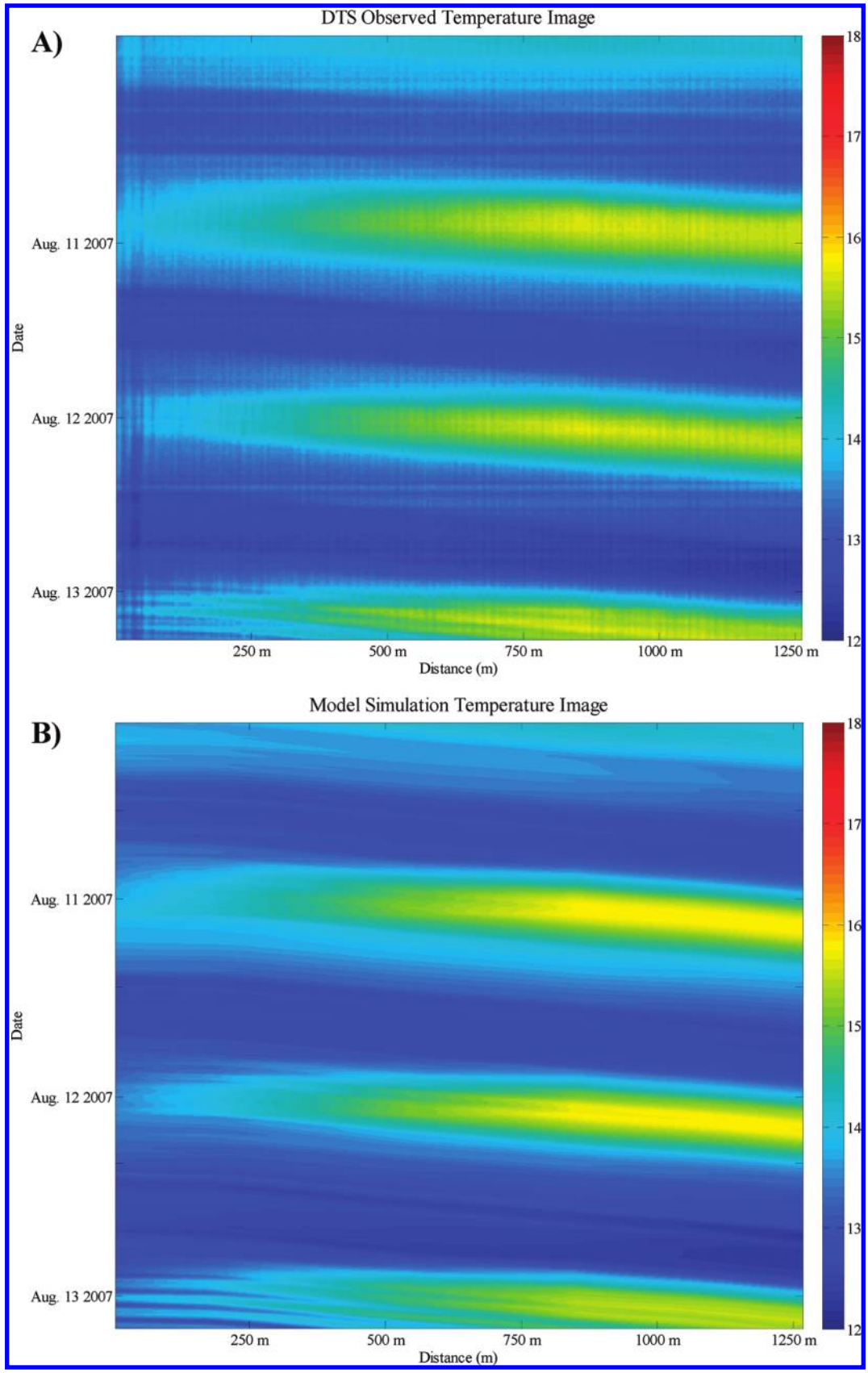


**FIGURE 2. (A) DTS observed temperature over the length of the stream and the duration of the experiment and (B) control simulation temperature over the same time frame. The visible temperature striations on August 13 are a result of upstream pumping. The color bar represents temperature in degrees Celsius.**

total radiation load and the gradient of relative humidity, and therefore, we see the highest evaporation within the open scenario and the least within the forest scenario. Direct incoming solar radiation and land cover longwave radiation are the driving components in the energy balance, which cause the temperature differences in these simulations. For

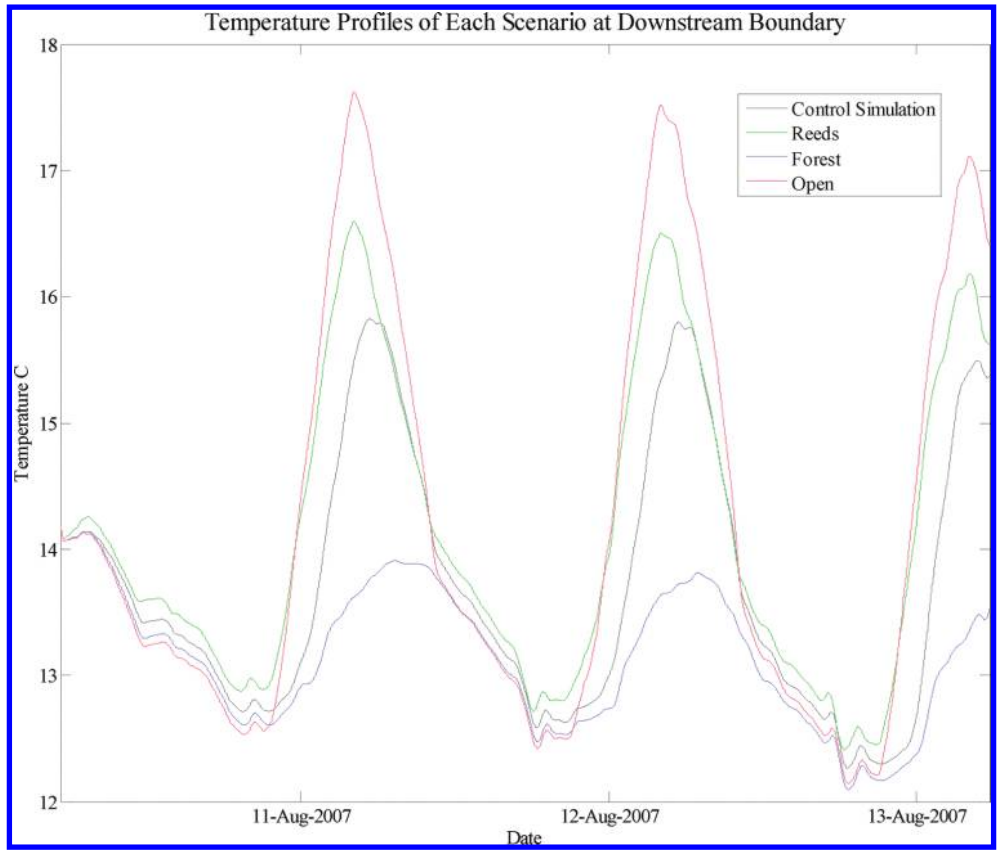


**FIGURE 3. Modeled stream temperature outputs at the downstream boundary of each vegetation cover scenario relative to the calibrated model simulation including the three sections of different vegetation type.**

**TABLE 2. Model Parameter Values for Each Land Use Scenario**

| | open | reeds | forest |
|---|---|---|---|
| $D_f$ | 0.34−0.35 | 0.17−0.18 | 0.15 |
| $\theta_{vts}$ | 1 | 0.9 | 0.975 |

example, the reeds scenario shows significantly higher land cover longwave radiation compared to the forest and open simulations. This is due to the differences in air temperature for each simulation and the $\theta_{vts}$ parameter (eq 4). While the $\theta_{vts}$ parameter varies little over the various scenarios (Table 2), it has a profound impact on in-stream temperatures, enforcing the notion that solar radiation is a first-order control to stream heating.

The mean peak air temperature, as measured by the SensorScope meteorological stations, for each section provided a 1.57 °C increase between the open and forest scenarios (Table 4) during our study period. The implication is that mature forest cover has influence on various microclimate forcings that drive the energy balance, such as wind speeds, humidity, and air temperature. Surface-emitted longwave (outgoing) and atmospheric longwave (incoming) fluxes essentially offset each other in all scenarios, leaving direct incoming solar radiation to account for 89−100% of total radiation load into the stream. This makes it the most significant term within the energy balance and subsequently the term that provides the most in-stream temperature change (Table 3). Solar radiation differences between simulations are also explained due to the $D_f$ coefficient used for the reed and forest scenarios in eq 2. $D_f$ is smaller in the forest than in the part with minimal reed cover. This is explained by the greater depth of water in the forest portion, as observed in the field. The relatively high $\theta_{vts}$ in the forest compared to the reeds section is explained by the distance between the vegetation and the water, which is far greater

**TABLE 3. Average Energy Balance Components at the Boiron River for Each Land Use Scenario[a]**

| | energy, W m$^{-2}$ | | | |
|---|---|---|---|---|
| | calibrated model | open | reeds | forest |
| direct incoming solar radiation ($SW_d$) | 129.33 | 273.65 | 163.29 | 43.23 |
| land cover longwave radiation ($LWR_l$) | 21.60 | 0 | 39.43 | 9.70 |
| surface emitted longwave radiation ($LW_s$) | −373.50 | −377.85 | −373.37 | −367.31 |
| atmospheric longwave radiation ($LW_{atm}$) | 367.16 | 371.25 | 368.35 | 361.62 |
| bed conduction (COND) | −3.25 | −0.44 | −3.55 | −7.14 |
| latent heat flux | −29.83 | −50.25 | −38.20 | −12.51 |
| sensible heat flux | 25.27 | 34.28 | 30.51 | 12.14 |
| total | 136.78 | 250.65 | 196.46 | 39.73 |

[a] For an afternoon period (2:30−4:30 p.m.) on August 11−13, 2007.

**TABLE 4. Stream Temperatures and Maximum Mean Air Temperature for Each Land Use Scenario over the Identical 3-Day Period in August 2007[a]**

| | stream temperature, °C | | | | |
|---|---|---|---|---|---|
| | max | min | mean max | mean min | mean max air temp, °C |
| DTS observed | 15.72 | 12.25 | 14.85 | 12.87 | 21.71 |
| calibrated model | 15.84 | 12.27 | 14.86 | 12.76 | 21.71 |
| Open | 17.62 | 12.15 | 15.58 | 12.68 | 22.21 |
| Reeds | 16.59 | 12.39 | 14.95 | 12.81 | 21.81 |
| Forest | 14.33 | 12.08 | 13.62 | 12.67 | 20.64 |

[a] Mean max is computed as the average temperature during the two peak hours (2:30−4:30 p.m.) and mean min is the average temperature during the two coolest hours (4:30−6:30 a.m.).

in the forest than within the reed section, and by the density of the reed cover.

DTS proved to be a useful and accurate method for stream temperature model validation. Extrapolating point measurements of stream temperatures can lead to misrepresentation of the stream temperature dynamics by assuming linear regression and not accounting for discrete changes within the stream profile. Precise stream temperature measurements in the continuum allowed for more robust model outcomes.

The influence of vegetation shading on peak high temperatures was shown to be appreciable and well captured in numerical simulations. Solar radiation was demonstrated to be a first-order control on stream temperatures for this stream, while outgoing longwave radiation from vegetation had a measurable effect. While mature forest canopy is the land-use management option that provided the greatest control of peak temperatures, in-stream reeds were shown to exhibit lower maximum stream temperatures than the open scenario and are potentially an interesting interim solution for stream temperature buffering. There are many non-temperature-related considerations in the choice of reeds versus forest—for instance, the effect on fish habitat, the oxygen budget, and nutrient balance of the stream—that would require careful attention as well. A common practice within this region in Switzerland is to remove in-stream vegetation, including reeds, which we predict increases stream temperature and may have other deleterious consequences on the habitat. Simple cessation of the dredging of reeds within the stream channel, what Kauffman et al. (*33*) call passive restoration, could greatly mitigate anthropogenic degradation if effects on sediment load, oxygen levels, and in-stream habitat are considered.

## Acknowledgments

This project was made possible in part through the National Science Foundation grant no. EAR 0711594, the Competence Center Environment and Sustainability of the ETH Domain (CCES) SwissEx, the National Center of Competence in Research: Mobile Information and Communication Systems (NCCR-MICS), and the European Commission 7th Framework Programme (FP7) grant no. 224416.

## Literature Cited

(1) Holtby, L. B. Effects of logging on stream temperatures in Carnation Creek, British Columbia, and associated impacts on the coho salmon (*Oncorhynchus kisutch*). *Can. J. Fish. Aquat. Sci.* **1988**, *45*, 502–515.

(2) Borman, M.; Larson, L. A case study of river temperature response to land use and environmental thermal patterns along a river in northeastern Oregon. *J. Soil Water Conserv.* **2003**, *58*, 8–12.

(3) Poole, G. C.; Berman, C. H. An ecological perspective on in-stream temperature: Natural heat dynamics and mechanisms of human-caused thermal degradation. *Environ. Manage.* **2001**, *27*, 787–802.

(4) Fitzgerald, D. G.; Kott, E.; Lanno, R. P.; Dixon, D. G. A quarter century of change in the fish communities of three small streams modified by anthropogenic activities. *J. Aquat. Ecosyst. Stress Recovery.* **1997**, *6* (2), 111–127.

(5) Brett, J. R. Some principles in thermal requirements of fishes. *Q. Rev. Biol.* **1956**, *31*, 75–87.

(6) Theurer, F. D.; Lines, I.; Nelson, T. Interaction between riparian vegetation, water temperature, and salmonid habitat in the Tucannon River. *Wat. Resour. Bull.* **1985**, *21*, 53–64.

(7) Marine, K. R.; Cech, J. J., Jr. Effects of high water temperature on growth, smoltification, and predator avoidance in juvenile Sacramento River Chinook salmon. *North Am. J. Fish. Manage.* **2004**, *24*, 198–210.

(8) Peterson, J. H.; Kitchell, J. F. Climate regimes and water temperature changes in the Columbia River: Bioenergetic implications for predators of juvenile salmon. *Can. J. Fish. Aquat. Sci.* **2001**, *58*, 1831–1841.

(9) Lee, R. M.; Rinne, J. N. Critical thermal maxima of five trout species in the south-western United States. *Trans. Am. Fish. Soc.* **1980**, *109*, 632–635.

(10) Johnson, S. L. Factors influencing stream temperatures in small streams: substrate effects and a shading experiment. *Can. J. Fish. Aquat. Sci.* **2004**, *61*, 913–923.

(11) Brown, G. W.; Krygier, J. T. Effects of clear-cutting on stream temperature. *Water Resour. Res.* **1970**, *6* (4), 1133–1139.

(12) Sinokrot, B. A.; Stefan, H. G. Stream temperature dynamics: measurements and modeling. *Water Resour. Res.* **1993**, *29* (7), 2299–2312.

(13) Webb, B. W.; Zhang, Y. Spatial and seasonal variability in the components of the river heat budget. *Hydrol. Processes* **1997**, *11*, 79–101.

(14) Johnson, S. L.; Jones, J. A. Stream temperature responses to forest harvest and debris flows in western Cascades, Oregon. *Can. J. Fish. Aquat. Sci.* **2000**, *57* (Suppl. 2), 30–39.

(15) Cox, T. J.; Rutherford, J. C. Thermal tolerances of two stream invertebrates exposed to diurnally varying temperature. *N. Z. J. Mar. Freshwater Res.* **2000**, *34*, 203–208.

(16) Chen, J.; Franklin, J. F.; Spies, T. A. Contrasting microclimates among clearcut, edge, and interior of old-growth Douglas-fir forest. *Agric. For. Meteorol.* **1993**, *63*, 219–237.

(17) Beschta, R. L. Riparian shade and stream temperature: An alternative perspective. *Rangelands* **1997**, *19* (2), 25–28.

(18) Mostovoy, G. V.; Anantharaj, V.; King, R. L.; Filippova, M. G. Interpretation of the relationship between skin temperature and vegetation fraction: Effect of subpixel soil temperature variability. *Int. J. Remote Sens.* **2008**, *29* (10), 2819–2831.

(19) Larson, L. L.; Larson, S. E. Riparian shade and stream temperature: A perspective. *Rangelands* **1996**, *18*, 149–152.

(20) Zwieniecki, M.; Newton, M. Influence of streamside cover and stream features on temperature trends in forested streams of western Oregon. *West. J. Appl. For.* **1999**, *14*, 106–112.

(21) Canton de Vaud (Switzerland) Project SAU. Available at http://www.vd.ch/fileadmin/user_upload/themes/environnement/eau/fichiers_pdf/SAU.pdf.

(22) Burkhardt-Holm, P.; Peter, A.; Segner, H. Project Fishnet: A balance between analysis and synthesis. *Aqua. Sci.* **2002**, *64*, 36–54.

(23) Boillat, S.; Rubin, J. F. Creation de caches a poisson dans le Boiron de Morges, *Assoc. Truite-Leman.* **2006**.

(24) Wahli, T.; Bernet, D.; Segner, H.; Schmidt-Posthaus, H. Role of altitude and water temperature as regulating factors for the geographical distribution of *Tetracapsuloides bryosalmonae* infected fishes in Switzerland. *J. Fish Biol.* **2008**, *73*, 2184–2197.

(25) Fischnetz. Dem Fischrückgang auf der Spur. Schlussbericht des Projekts Netzwerk Fischrückgang Schweiz. EAWAG (Swiss Federal Institute for Environmental Science and Technology), Dübendorf, Switzerland, and BUWAL (Swiss Agency for the Environment, Forests and Landscape), Bern, Switzerland, 2004.

(26) Jakob, A. Temperaturentwicklung in den fliessgewässern. *BUWAL Mitt. Fisch.* **1998**, *66*, 29–40.

(27) Burkhardt-Holm, P.; Giger, W.; Guttinger, H.; Oschenbein, U.; Peter, A.; Scheurer, K.; Segner, H.; Staub, E.; Suter, M. Where have all the fish gone? *Environ. Sci. Technol.* **2005**, *39* (21), 441A–447A.

(28) Selker, J. S.; Thévenaz, L.; Huwald, H.; Mallet, A.; Luxemburg, W.; van de Giesen, N.; Stejskal, M.; Zeman, J.; Westhoff, M.; Parlange, M. B. Distributed fiber optic temperature sensing for hydrologic systems. *Water Resour. Res.* **2006**, *42* (12), 8.
(29) Selker, J. S.; van de Giesen, N.; Westhoff, M.; Luxemburg, W.; Parlange, M. Fiber optics opens window on stream dynamics. *Geophys. Res. Lett.* **2006b**, *33* (24), 4.
(30) Westhoff, M. C.; Savenije, H. H. G.; Luxemburg, W.; Stelling, J G. S.; van de Giesen, N.; Selker, J. S.; Pfister, L.; Uhlenbrook, S. A distributed stream temperature model using high resolution temperature observations. *Hydrol. Earth Syst. Sci.* **2007**, *11*, 1469–1480.
(31) Monteith, J. L. Evaporation and surface temperature. *Q. J. R. Meteorol. Soc.* **1981**, *107*, 1–27.
(32) Mobley, C. D. In *In Light and Water: Radiative transfer in natural waters*; Academic Press: New York, 1994.
(33) Kauffman, J. B.; Beschta, R. L.; Otting, N.; Lytjen, D. An ecological perspective of riparian and stream restoration in the western United States. *Fisheries* **1997**, *22* (5), 12–24.

ES902654F